Nonlinear Legendre Spectral Finite Elements for Wind Turbine Blade Dynamics

Qi Wang[*1], Michael A. Sprague[†1], Jason Jonkman[‡1] and Nick Johnson[§2]

[1]National Renewable Energy Laboratory, Golden, CO 80401
[2]Department of Mechanical Engineering, Colorado School of Mines, Golden, CO 80401

This paper presents a numerical implementation and examination of new wind turbine blade finite element model based on Geometrically Exact Beam Theory (GEBT) and a high-order spectral finite element method. The displacement-based GEBT is presented, which includes the coupling effects that exist in composite structures and geometric nonlinearity. Legendre spectral finite elements (LSFEs) are high-rder finite elements with nodes located at the Gauss-Legendre-Lobatto points. LSFEs can be an order of magnitude more efficient that low-order finite elements for a given accuracy level. The new LSFE code is implemented in the new FAST Modularization Framework for dynamic simulation of highly flexible composite-material wind turbine blades. The framework allows for fully interactive simulations of turbine blades in operating conditions. Numerical examples showing validation and LSFE performance are provided in the numerical examples section. It concludes that the implemented code can be used as a efficient high-fidelity beam tool in FAST.

I.   Introduction

Wind power is becoming one of the most important renewable-energy sources in the United States. In recent years, the size of wind turbines has been increasing immensely to lower the cost, which, because of weight restrictions, also leads to highly flexible turbine blades. This huge electro-mechanical system poses a significant challenge for engineering design and analysis. Although possible with modern super computers, direct three-dimensional (3D) structural analysis is so computationally expensive that engineers are always seeking for efficient high-fidelity simplified models.

Beam models are widely used to represent and analyze engineering structures that have one of its dimensions much larger than the other two. Many engineering components can be idealized as beams: bridges in civil engineering, joists and lever arms in heavy-machine industries, and helicopter rotor blades. The blades, tower, and shaft in a wind turbine system can be considered as beams. In the weight-critical applications of beam structures, like high-aspect-ratio wings in aerospace and wind energy, composite materials are attractive due to their superior strength-to-weight and stiffness-to-weight ratios. However, analysis of composite-materials structures is more difficult than their isotropic counterparts due to elastic-coupling effects. The geometrically exact beam theory (GEBT) first first proposed by Reissner[2], is a method that has proven powerful for analysis of highly flexible composite beams in the helicopter engineering community. During the past several decades, much effort has been invested in this area. Simo[3] and Simo and Vu-Quoc[4] extended Reissner's work to deal with three-dimensional (3D) dynamic problems. Jelenić and Crisfield[5] implemented this theory using the finite-element method where a new approach for interpolating the rotation field was proposed that preserves the geometric exactness. Betsch and Steinmann[6] circumvented the interpolation of rotation by introducing a re-parameterization of the weak form corresponding to the equations of motion of GEBT. It is noted that Ibrahimbegović and his colleagues implemented this theory for static[7] and dynamic[8] analysis. In contrast to the displacement-based implementations, the geometric exact beam theory has also been formulated by mixed finite elements where both the primary and dual field are independently interpolated[9]. In the mixed formulation, all of the necessary ingredients, including Hamilton's principle and kinematic equations, are combined in a single variational formulation statement; Lagrange multipliers, motion variables, generalized strains, forces and moments, linear and angular momenta, and displacement and rotation variables are considered as independent quantities. Yu et al.[10,11] presented the implementation of GEBT in a mixed formulation; various rotation parameters were investigated and the code was validated against analytical and numerical solutions. Readers are referred to Hodges[12], where comprehensive derivations and discussions on nonlinear composite-beam theories can be found.

Legendre spectral finite elements[13,14] (LSFEs) are p-type finite elements whose shape functions are Lagrangian interpolants with node locations at the Gauss-Lobatto-Legendre (GLL) points. LSFEs combine the accuracy of global

---

American Institute of Aeronautics and Astronautics

spectral methods with geometric flexibility of h-type FEs. The spectral FEs have seen successful use in the simulation of fluid dynamics [13–15], two-dimensional elastic wave propagation in solid media in geophysics [16], elastodynamics [17], and acoustic wave propagation [18]. However, it has seen limited application to dynamic analysis of beam [19–22] and plate elements [23–25]. COMMENT: we need to add references on "quadrature elements"

In this paper, we present a displacement-based implementation of geometrically exact beam theory using LSFEs. This work builds on a previous effort which showed the implementation of three-dimensional rotation parameters [11] and a demonstration example of two-dimensional nonlinear spectral beam elements [26] for static deformation. The code implemented in this work is in accordance to FAST Modularization Framework [27], which allows simulation of a whole turbine under realistic operating conditions. COMMENT: EXPAND ON FAST MODULARIZATION

The paper is organized as follows. The theoretical foundation of the geometrically exact beam theory is introduced first. Then the GEBT discretization by LSFEs is discussed. Finally, verification examples are provided to show the accuracy and efficiency of the GEBT LSFEs for isotropic and composite beams.

II.   Geometrically Exact Beam Theory

For completeness, this section reviews the geometrically exact beam theory and linearization process of the governing equations. The content of this section can be found in many other papers and textbooks. Figure 1 shows a beam in its initial undeformed and deformed states. A reference frame $\mathbf{b}_i$ is introduced along the beam axis for the undeformed state; a frame $\mathbf{B}_i$ is introduced along each point of the deformed beam axis. Curvilinear coordinate x_1 defines the intrinsic parameterization of the reference line. In this paper, we use matrix notation to denote vectorial or
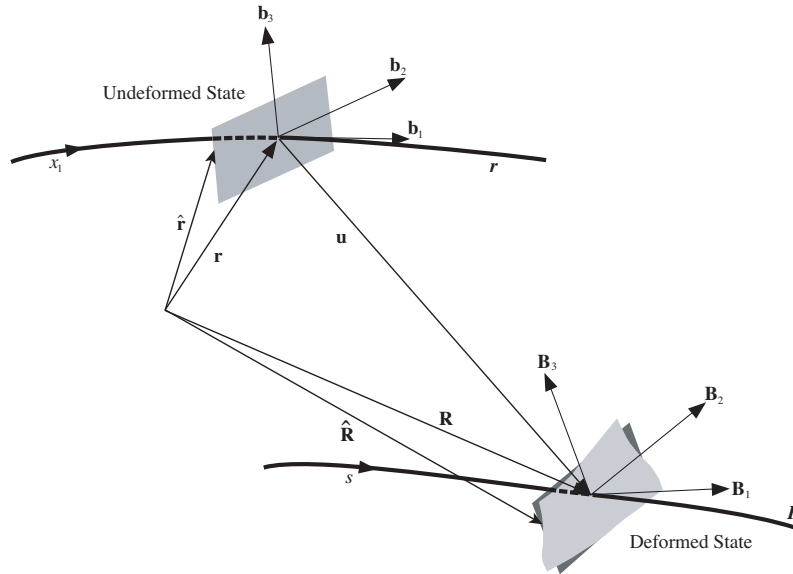

Figure 1: Schematic of beam deformation

vectorial-like quantities. For example, we use a underline to denote a vector $\underline{u}$, a bar to denote unit vector $\bar{n}$, and double underline to denote a tensor $\underline{\underline{\Delta}}$. Note that sometimes the underlines only denote the dimension of the corresponding matrix. The governing equations of motion for geometric exact beam theory can be written as [28]

$$\dot{\underline{h}} - \underline{F}' = \underline{f} \tag{1}$$

$$\dot{\underline{g}} + \dot{\tilde{u}}\underline{h} - \underline{M}' - (\tilde{x}_0' + \tilde{u}')\underline{F} = \underline{m} \tag{2}$$

where $\underline{h}$ and $\underline{g}$ are the linear and angular momenta resolved in the inertial coordinate system, respectively; $\underline{F}$ and $\underline{M}$ are the beam's sectional forces and moments, respectively; $\underline{u}$ is the 1D displacement of the reference line; $\underline{x}_0$ is the initial position vector of a point along the beam's reference line; $\underline{f}$ and $\underline{m}$ are the distributed force and moment applied to the beam structure. Notation $(\bullet)'$ indicates a derivative with respect to the beam axis x_1 and $\dot{(\bullet)}$ indicates a derivative with respect to time. The tilde operator $\widetilde{(\bullet)}$ defines a second-order, skew-symmetric tensor corresponding to the given vector. In the literature, it is also termed as "cross-product matrix". For example,

$$\widetilde{n} = \begin{bmatrix} 0 & -n_3 & n_2 \\ n_3 & 0 & -n_1 \\ -n_2 & n_1 & 0 \end{bmatrix}$$

American Institute of Aeronautics and Astronautics

The constitutive equations relate the velocities to the momenta and the one-dimensional strain measures to the sectional resultants as

$$\left\{\frac{\underline{h}}{\underline{g}}\right\} = \underline{\underline{\mathcal{M}}}\left\{\frac{\dot{\underline{u}}}{\underline{\omega}}\right\} \tag{3}$$

$$\left\{\frac{\underline{F}}{\underline{M}}\right\} = \underline{\underline{\mathcal{C}}}\left\{\frac{\underline{\epsilon}}{\underline{\kappa}}\right\} \tag{4}$$

where $\underline{\underline{\mathcal{M}}}$ and $\underline{\underline{\mathcal{C}}}$ are the 6×6 sectional mass and stiffness matrices,respectively, note that they are not really tensors; $\underline{\epsilon}$ and $\underline{\kappa}$ are the 1D strains and curvatures, respectively. $\underline{\omega}$ is the angular velocity vector that is defined by the rotation tensor $\underline{\underline{R}}$ as $\underline{\omega} = \mathrm{axial}(\dot{\underline{\underline{R}}}\,\underline{\underline{R}})$.

For a displacement-based finite element implementation, there are six degree-of-freedoms(DoFs) at each node: 3 displacement components and 3 rotation components. Here we use $\underline{q}$ to denote the elemental displacement array as $\underline{q} = \begin{bmatrix} \underline{u}^T & \underline{p}^T \end{bmatrix}$ where $\underline{u}$ is the 1D displacement and $\underline{p}$ is the rotation parameter vector. The acceleration array can thus be defined as $\underline{a} = \begin{bmatrix} \ddot{\underline{u}}^T & \dot{\underline{\omega}}^T \end{bmatrix}$. For nonlinear finite element analysis, the discretized and incremental forms of displacement, velocity, and acceleration array are written as

$$\underline{q}(x_1) = \underline{\underline{N}}\,\hat{\underline{q}} \quad \Delta \underline{q}^T = \begin{bmatrix} \Delta \underline{u}^T & \Delta \underline{p}^T \end{bmatrix} \tag{5}$$

$$\underline{v}(x_1) = \underline{\underline{N}}\,\hat{\underline{v}} \quad \Delta \underline{v}^T = \begin{bmatrix} \Delta \dot{\underline{u}}^T & \Delta \underline{\omega}^T \end{bmatrix} \tag{6}$$

$$\underline{a}(x_1) = \underline{\underline{N}}\,\hat{\underline{a}} \quad \Delta \underline{a}^T = \begin{bmatrix} \Delta \ddot{\underline{u}}^T & \Delta \dot{\underline{\omega}}^T \end{bmatrix} \tag{7}$$

where $\underline{\underline{N}}$ is the shape function matrix and $(\hat{\bullet})$ denotes a column matrix of nodal values. The governing equations for beams are highly nonlinear so that a linearization process is needed. According to Ref[28], the linearized governing equations in Eq. (1) and (2) are in the form of

$$\hat{\underline{\underline{M}}}\Delta\hat{\underline{a}} + \hat{\underline{\underline{G}}}\Delta\hat{\underline{v}} + \hat{\underline{\underline{K}}}\Delta\hat{\underline{q}} = \hat{\underline{F}}^{ext} - \hat{\underline{F}} \tag{8}$$

where the $\hat{\underline{\underline{M}}}$, $\hat{\underline{\underline{G}}}$, and $\hat{\underline{\underline{K}}}$ are the elemental mass, gyroscopic, and stiffness matrices, respectively; $\hat{\underline{F}}$ and $\hat{\underline{F}}^{ext}$ are the elemental forces and externally applied loads, respectively. They are defined as follows

$$\hat{\underline{\underline{M}}} = \int_0^l \underline{\underline{N}}^T \underline{\underline{\mathcal{M}}}\,\underline{\underline{N}}dx_1 \tag{9}$$

$$\hat{\underline{\underline{G}}} = \int_0^l \underline{\underline{N}}^T \underline{\underline{\mathcal{G}}}^I\,\underline{\underline{N}}dx_1 \tag{10}$$

$$\hat{\underline{\underline{K}}} = \int_0^l \left[\underline{\underline{N}}^T (\underline{\underline{\mathcal{K}}}^I + \underline{\underline{\mathcal{Q}}})\,\underline{\underline{N}} + \underline{\underline{N}}^T \underline{\underline{\mathcal{P}}}\,\underline{\underline{N}}' + \underline{\underline{N}}'^T \underline{\underline{\mathcal{C}}}\,\underline{\underline{N}}' + \underline{\underline{N}}'^T \underline{\underline{\mathcal{O}}}\,\underline{\underline{N}} \right] dx_1 \tag{11}$$

$$\hat{\underline{F}} = \int_0^l (\underline{\underline{N}}^T \underline{\mathcal{F}}^I + \underline{\underline{N}}^T \underline{\mathcal{F}}^D + \underline{\underline{N}}'^T \underline{\mathcal{F}}^C)dx_1 \tag{12}$$

$$\hat{\underline{F}}^{ext} = \int_0^l \underline{\underline{N}}^T \underline{\mathcal{F}}^{ext}dx_1 \tag{13}$$

The new matrix notations in Eq. (9) to (13) are briefly introduced here. $\underline{\underline{\mathcal{M}}}$ is the sectional mass matrix resolved in inertial system; $\underline{\mathcal{F}}^C$ and $\underline{\mathcal{F}}^D$ are elastic forces obtained from Eq. (1) and (2) as

$$\underline{\mathcal{F}}^C = \left\{\frac{\underline{F}}{\underline{M}}\right\} = \underline{\underline{\mathcal{C}}}\left\{\frac{\underline{\epsilon}}{\underline{\kappa}}\right\} \tag{14}$$

$$\underline{\mathcal{F}}^D = \begin{bmatrix} \underline{\underline{0}} & \underline{\underline{0}} \\ (\tilde{x}_0' + \tilde{u}')^T & \underline{\underline{0}} \end{bmatrix} \underline{\mathcal{F}}^C \equiv \underline{\underline{\Upsilon}}\,\underline{\mathcal{F}}^C \tag{15}$$

where $\underline{0}$ denotes a 3×3 null matrix. The $\underline{\underline{\mathcal{G}}}^I$, $\underline{\underline{\mathcal{K}}}^I$, $\underline{\underline{\mathcal{O}}}$, $\underline{\underline{\mathcal{P}}}$, $\underline{\underline{\mathcal{Q}}}$, and $\underline{\mathcal{F}}^I$ in Eq. (10), Eq. (11), and Eq. (12) are defined as

$$\underline{\underline{\mathcal{G}}}^I = \begin{bmatrix} \underline{\underline{0}} & (\tilde{\omega}m\eta)^T + \tilde{\omega}m\tilde{\eta}^T \\ \underline{\underline{0}} & \tilde{\omega}\underline{\underline{\varrho}} - \widetilde{\underline{\underline{\varrho}}\omega} \end{bmatrix} \tag{16}$$

$$\underline{\underline{\mathcal{K}}}^I = \begin{bmatrix} \underline{\underline{0}} & \dot{\tilde{\omega}}m\tilde{\eta}^T + \tilde{\omega}\tilde{\omega}m\tilde{\eta}^T \\ \underline{\underline{0}} & \ddot{\tilde{u}}m\tilde{\eta} + \underline{\underline{\varrho}}\dot{\tilde{\omega}} - \widetilde{\underline{\underline{\varrho}}\dot{\omega}} + \tilde{\omega}\underline{\underline{\varrho}}\tilde{\omega} - \tilde{\omega}\widetilde{\underline{\underline{\varrho}}\omega} \end{bmatrix} \tag{17}$$

$$\underline{\underline{\mathcal{O}}} = \begin{bmatrix} \underline{\underline{0}} & \underline{\underline{C}}_{11}\tilde{E}_1 - \tilde{F} \\ \underline{\underline{0}} & \underline{\underline{C}}_{21}\tilde{E}_1 - \tilde{M} \end{bmatrix} \tag{18}$$

$$\underline{\underline{\mathcal{P}}} = \begin{bmatrix} \underline{\underline{0}} & \underline{\underline{0}} \\ \tilde{F} + (\underline{\underline{C}}_{11}\tilde{E}_1)^T & (\underline{\underline{C}}_{21}\tilde{E}_1)^T \end{bmatrix} \tag{19}$$

$$\underline{\underline{\mathcal{Q}}} = \underline{\underline{\Upsilon}}\,\underline{\underline{\mathcal{O}}} \tag{20}$$

$$\underline{\mathcal{F}}^I = \begin{Bmatrix} m\ddot{u} + (\dot{\tilde{\omega}} + \tilde{\omega}\tilde{\omega})m\eta \\ m\tilde{\eta}\ddot{u} + \underline{\underline{\varrho}}\dot{\omega} + \tilde{\omega}\underline{\underline{\varrho}}\omega \end{Bmatrix} \tag{21}$$

The following notations were introduced to simply the writing of the above expressions

$$\underline{E}_1 = \underline{x}_0' + \underline{u}' \tag{22}$$

$$\underline{\underline{C}} = \begin{bmatrix} \underline{\underline{C}}_{11} & \underline{\underline{C}}_{12} \\ \underline{\underline{C}}_{21} & \underline{\underline{C}}_{22} \end{bmatrix} \tag{23}$$

The derivation and linearization of governing equations of geometrically exact beam theory can be found in Ref[28].

III.   Legendre Spectral Finite Elements

The displacement fields in a element are interpolated as

$$\underline{u}(s) = h^k(s)\underline{\hat{u}}^k \tag{24}$$

$$\underline{u}'(s) = h^{k\prime}(s)\underline{\hat{u}}^k \tag{25}$$

where $h^k(s)$ is the Lagrangian-interpolan shape function of node k, $k = 1, 2, ..., n + 1$, where n is the polynomial order of of the basis functions, and $\underline{\hat{u}}^k$ is the kth nodal value. However, as discussed in Ref[29], the three-dimensional rotation field cannot be simply interpolated as the displacement field in the form of

$$\underline{c}(s) = h^k(s)\underline{\hat{c}}^k \tag{26}$$

$$\underline{c}'(s) = h^{k\prime}(s)\underline{\hat{c}}^k \tag{27}$$

where $\underline{c}$ is the rotation field in a element and $\underline{\hat{c}}^k$ is the nodal value at the kth node, for three reasons: 1) rotations do not form a linear space so that they must be "composed" instead of added; 2) a rescaling operation is needed to eliminate the singularity existing in the vectorial rotation parameters; 3) the rotation field lacks objectivity, which, as defined by Crisfield and Jelenić[5], refers to the invariance of strain measures computed through interpolation to the addition of a rigid-body motion. Therefore, we adopt the more robust interpolation approach proposed by Crisfield and Jelenić[5] to deal with the finite rotations. Our approach is described as follows

Step 1: Compute the nodal relative rotations, $\underline{\hat{r}}^k$ by removing the rigid body rotation, $\underline{\hat{c}}^1$, from the finite rotation at each node, $\underline{\hat{r}}^k = \underline{\hat{c}}^{1-} \oplus \underline{\hat{c}}^k$.

Step 2: Interpolate the relative rotation field: $\underline{r}(s) = h^k(s)\underline{\hat{r}}^k$ and $\underline{r}'(s) = h^{k\prime}(s)\underline{\hat{r}}^k$. Find the curvature field $\underline{\kappa}(s) = \underline{\underline{R}}(\underline{\hat{c}}^1)\underline{\underline{H}}(\underline{r})\underline{r}'$.

Step 3: Restore the rigid body rotation removed in Step 1: $\underline{c}(s) = \underline{\hat{c}}^1 \oplus \underline{r}(s)$.

where H is the tangent tensor that relates the curvature vector k and rotation vector p as

$$\underline{k} = \underline{\underline{H}}\,\underline{p}' \tag{28}$$

In the LSFE approach, shape functions (e.g., those composing $\underline{N}$) are n^{th}-order Lagrangian interpolants, where nodes are located at the $n + 1$ GLL-quadrature points in the $[-1, 1]$ element natural-coordinate domain. Need more work here: a figure shows some LS elements (non-evenly placed internal nodes) and a short discussion of its advantages. The implementation of GEBT into the FE code, BeamDyn, carries out the integration in the space domain by using reduced Gauss quadrature. Time integration is performed using generalized-α scheme, which is a unconditionally stable, second-order accurate algorithm. More details regarding on the generalized-α method can be found in Ref[28,30]

American Institute of Aeronautics and Astronautics

IV. Numerical Examples

A. Example 1: Static bending of a cantilever beam

The first example is a benchmark problem for geometrically nonlinear analysis of beams[3,31]. We calculate the static deflection of a cantilever beam that is subjected at its free end to a constant moment M. The length of the beam L is $10\,in$ and the cross-sectional stiffness matrix is given below:

$$C^* = 10^3 \times \begin{bmatrix} 1770 & 0 & 0 & 0 & 0 & 0 \\ & 1770 & 0 & 0 & 0 & 0 \\ & & 1770 & 0 & 0 & 0 \\ & & & 8.16 & 0 & 0 \\ & & & & 86.9 & 0 \\ & & & & & 215 \end{bmatrix} \tag{29}$$

It is pointed out that the term with a asterisk denotes it is resolved in the material coordinate system. A sketch of this case can be found in Figure 2. The load applied at the tip is given by the following equation:
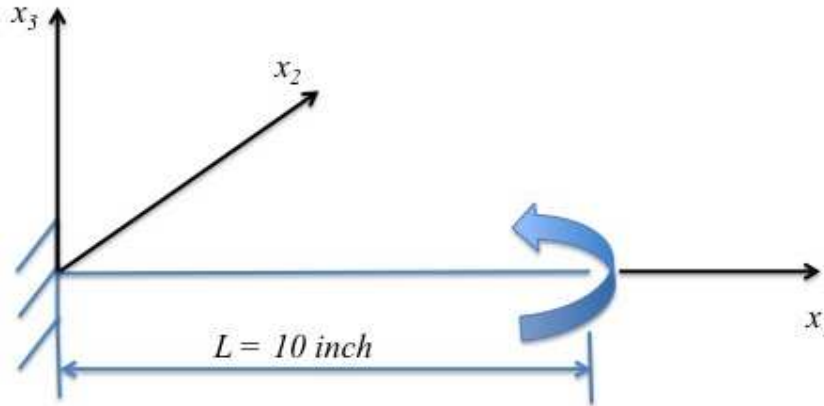
Figure 2: Sketch of a cantilever beam.

$$M_2 = \lambda \bar{M}_2 \tag{30}$$

where $\bar{M}_2 = \pi \frac{EI_2}{L}$. The parameter λ will vary between 0 and 2. In this case, the beam is discretized with two 5th order elements. The deformations of the beam are shown in Figure 3. The calculated results are compared with the
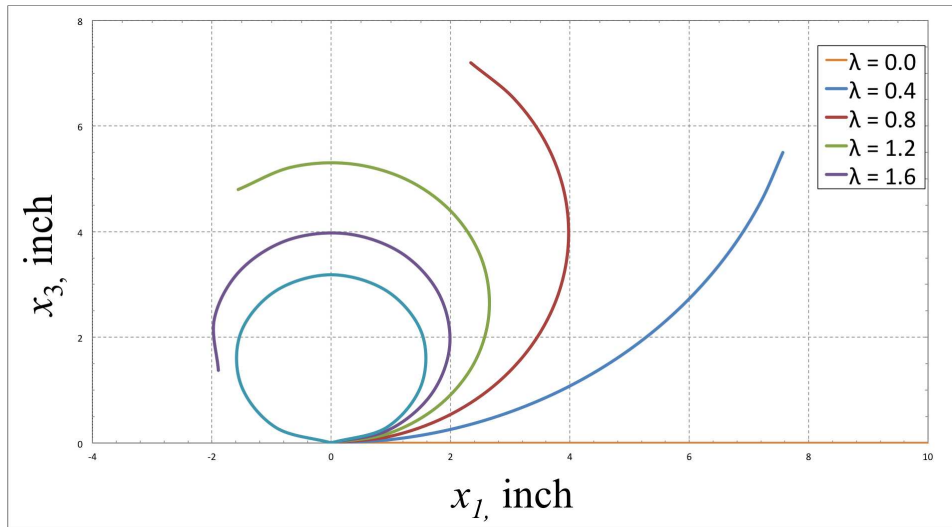
Figure 3: Deformations of a cantilever beam under several constant bending moments.

American Institute of Aeronautics and Astronautics

Table 1: Axial displacement u_1 of a cantilever beam subject to a constant moment (in inches).

λ	Analytical	BeamDyn	% Error
0.4	-2.4317	-2.4317	0.00
0.8	-7.6613	-7.6613	0.00
1.2	-11.5591	-11.5591	0.00
1.6	-11.8921	-11.8921	0.00
2.0	-10.0000	-10.0000	0.00

Table 2: Vertical displacement u_3 of a cantilever beam subject to a constant moment (in inches).

λ	Analytical	BeamDyn	% Error
0.4	5.4987	5.4987	0.00
0.8	7.1978	7.1979	0.0013
1.2	4.7986	4.7986	0.00
1.6	1.3747	1.3747	0.00
2.0	0.0000	0.0000	0.00

analytical solution, which can be found in Ref. [32] as

$$u_1 = \rho sin\left(\frac{x_1}{\rho}\right) - x_1 \quad u_3 = \rho\left(1 - cos\left(\frac{x_1}{\rho}\right)\right) \tag{31}$$

The results can be found in Table 1 and 2, respectively. Good agreement can be observed between these two sets of results.

The rotation parameters at each node along beam axis x_1 obtained from BeamDyn are plotted in Figure 4 for $\lambda = 0.8$ and $\lambda = 2.0$, respectively. It is noted that the three-dimensional rotations are represented by Wiener-Milenković parameter defined in the following equation:

$$\underline{p} = 4tan\frac{\phi}{4}\bar{n} \tag{32}$$

where ϕ is the rotation angle and $\bar{n}$ is the unit vector of rotation axis. The singularity exists in the above definition can be removed by a rescaling operation, which can be observed in Figure 4. Figure 5 shows the normalized error
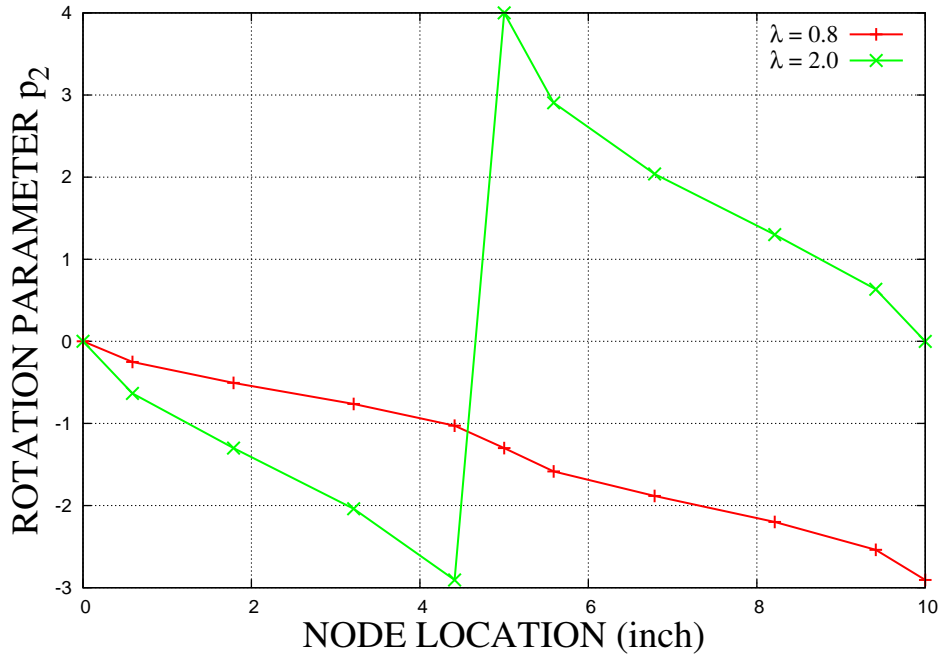

Figure 4: Wiener-Milenković rotation parameters along beam axis x_1 .

$\epsilon(u)$, where u is the tip displacement (at $x = L$), as a function of the number of model nodes for the calculation with

Table 3: Tip displacements and rotation parameters of a composite beam in Example 2

	u_1	u_2	u_3	p_1	p_2	p_3
BeamDyn	-0.09064	-0.06484	1.22998	0.18445	-0.17985	0.00488
Dymore	-0.09064	-0.06483	1.22999	0.18443	-0.17985	0.00488

Dymore quadratic elements (QE) and a single Legendre spectral element (LSE), where

$$\epsilon(u) = \left| \frac{u - u^a}{u^a} \right| \tag{33}$$

and u is the test solution and u^a is the analytical solution. The parameter λ is set to 1.0 for this case. The Legendre spectral elements (with p-refinement) exhibit highly desirable exponential convergence to machine precision error.

(a) u_1 　　　　　　　　　 (b) u_3
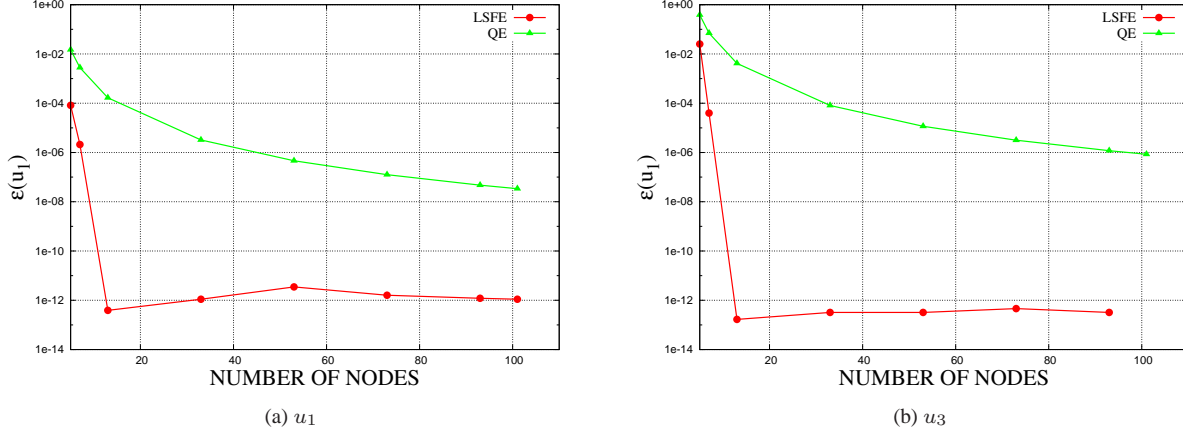
Figure 5: Normalized error of the (a) u_1 and (b) u_3 displacements as a function of the total number of nodes

B. Example 2: Static analysis of a composite beam

The second example is to show the capability of BeamDyn for composite beams with elastic couplings. The cantilever beam used in this case is 10 inches long with a boxed cross-section made of composite materials that can be found in Ref.[33]. Readers are referred to Figure 2 for sketch of this example. The stiffness matrix is given as

$$C^* = 10^3 \times \begin{bmatrix} 1368.17 & 0 & 0 & 0 & 0 & 0 \\ 0 & 88.56 & 0 & 0 & 0 & 0 \\ 0 & 0 & 38.78 & 0 & 0 & 0 \\ 0 & 0 & 0 & 16.96 & 17.61 & -0.351 \\ 0 & 0 & 0 & 17.61 & 59.12 & -0.370 \\ 0 & 0 & 0 & -0.351 & -0.370 & 141.47 \end{bmatrix} \tag{34}$$

A concentrated force $P = 150$ lbs along x_3 direction is applied at the free tip. In BeamDyn analysis, the beam is meshed with two 5th order elements. The displacements and rotation parameters at each node along beam axis are plotted in Figure 6. It is noted that the coupling effects exist between twist and two bendings. The applied in-plane force leads to a fairly large twist angle due to the bending-twist coupling, which can be observed in Figure. 6b. It is also noted that the internal nodes of Legendre Spectral Finite Elements are not evenly placed, which is different from conventional elements.

The tip displacements and rotations are compared with those obtained by Dymore in Table 3 for verification, where the beam is meshed with 10 3rd order elements. Good agreement can be observed between BeamDyn and Dymore results.

C. Example 3: dynamic analysis of a composite beam under sinusoidal force at the tip

The last example is a transient analysis of a composite beam with boxed cross-section that is used in Example 2. The beam has the same geometry and boundary conditions as the one in previous example. The mass sectional properties
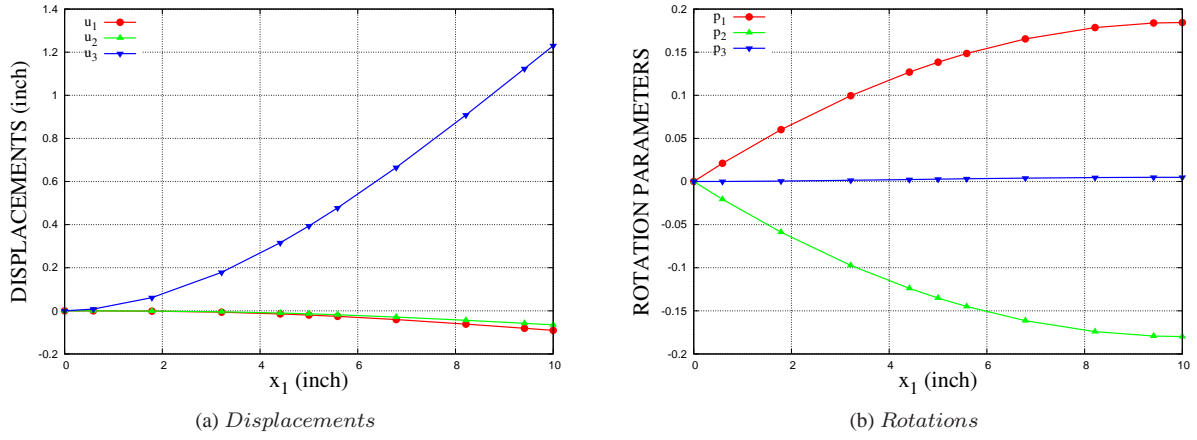
American Institute of Aeronautics and Astronautics

(a) *Displacements*

(b) *Rotations*

Figure 6: Displacements and rotation parameters along beam axis for Example 2.

are given by VABS[33,34] as

$$M^* = 10^{-2} \times \begin{bmatrix} 8.538 & 0 & 0 & 0 & 0 & 0 \\ 0 & 8.538 & 0 & 0 & 0 & 0 \\ 0 & 0 & 8.538 & 0 & 0 & 0 \\ 0 & 0 & 0 & 1.4433 & 0 & 01 \\ 0 & 0 & 0 & 0 & 0.40972 & 0 \\ 0 & 0 & 0 & 0 & 0 & 1.0336 \end{bmatrix} \tag{35}$$

The beam is divided into two 5th order elements in the current calculation and a sinusoidal point force is applied at the free tip in the x_3 direction given as

$$P = A_F \, sin(\omega_F \, t) \tag{36}$$

where $A_F = 1.0 \times 10^2 \, lbs$ and $\omega_F = 10 \, rad/s$ (see Figure 7). The time step used in this example is $0.005 \, s$ so that a set of converged results can be achieved. The tip displacement and rotation histories of the beam are plotted in Figure 8. Note that all the components, including three displacements and three rotations, are non-zero due to the elastic coupling effects. The time histories of the stress resultants at the root of the beam are given in Figure 9.
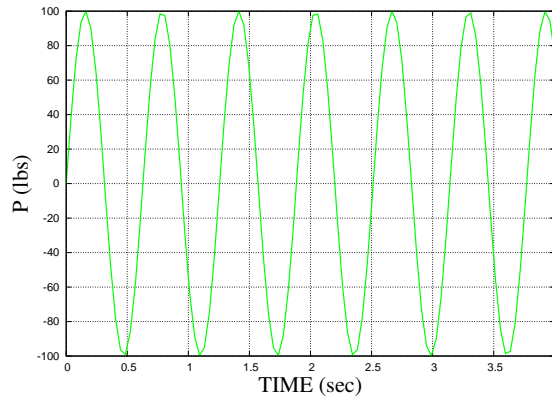
Figure 7: The sinusoidal vertical force in Example 3 .

V.   Conclusion

This paper presents a displacement-based implementation of geometrically exact beam theory. The Legendre spectral finite elements are adopted to discretize the beam in the space domain. Numerical examples were presented that demonstrate the capability of BeamDyn, a beam solver for wind turbine analysis developed by NREL. A benchmark static problem for nonlinear beam was studied first. The agreement between the results calculated by BeamDyn and analytical solution are excellent. Moreover, a convergence study has been conducted where the convergence rate of
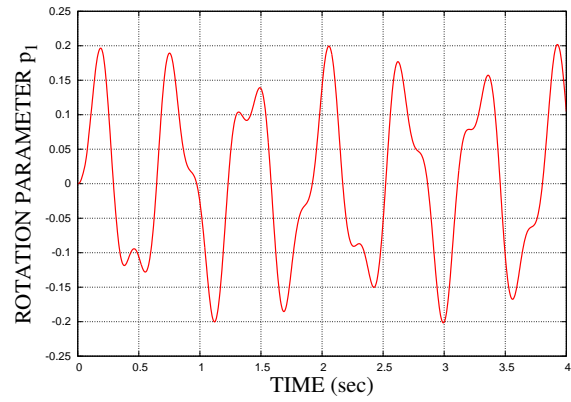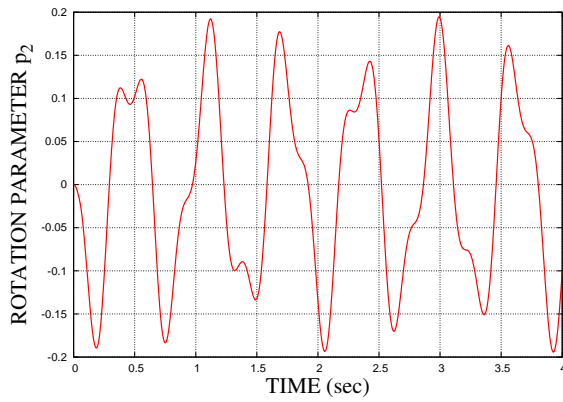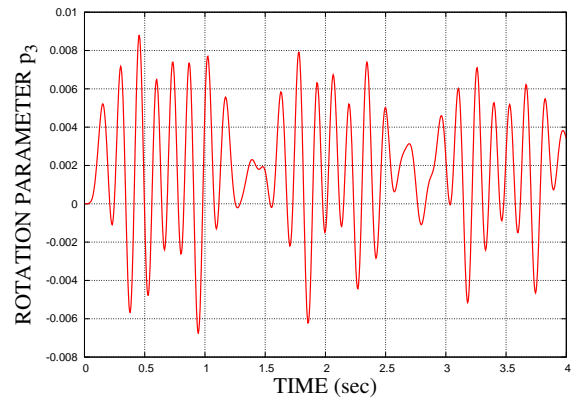
American Institute of Aeronautics and Astronautics
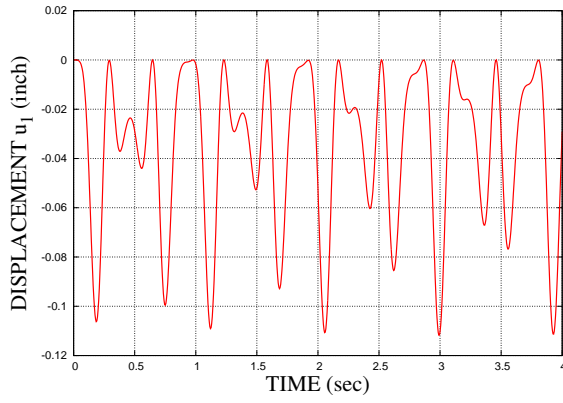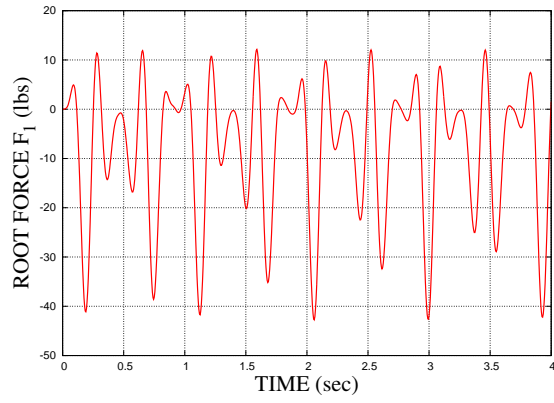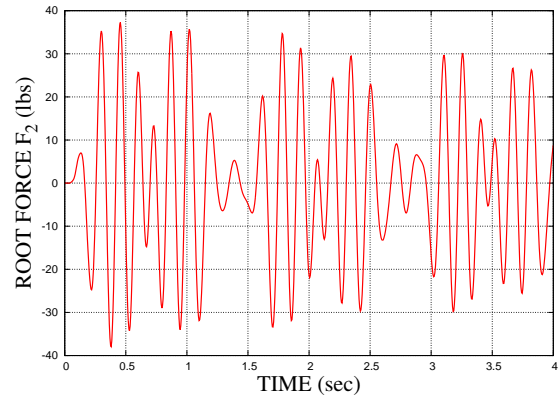
(a) u_1
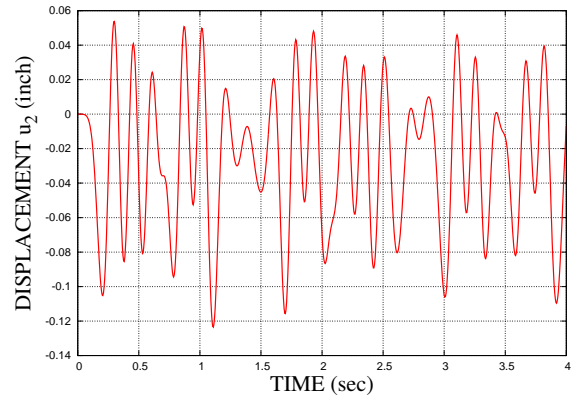
(b) u_2
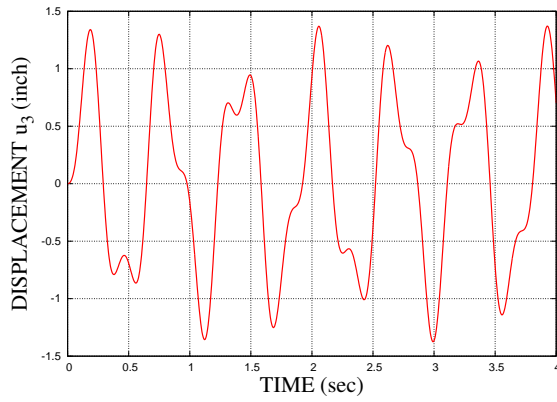
(c) u_3

(d) p_1

(e) p_2

(f) p_3
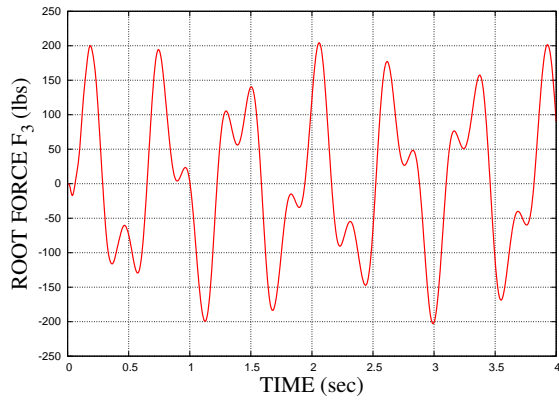
Figure 8: Tip displacement and rotation histories of a composite beam under vertical load.

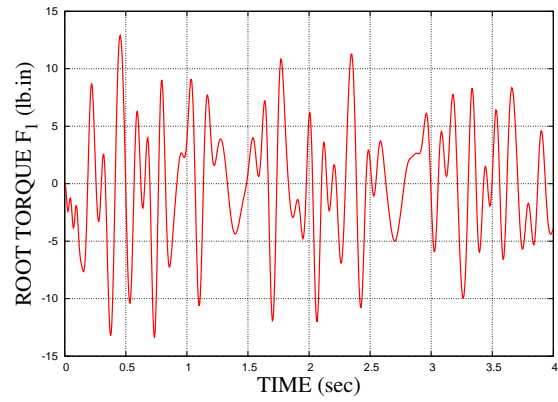American Institute of Aeronautics and Astronautics
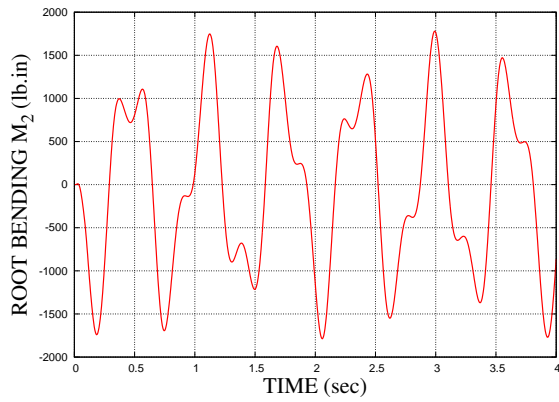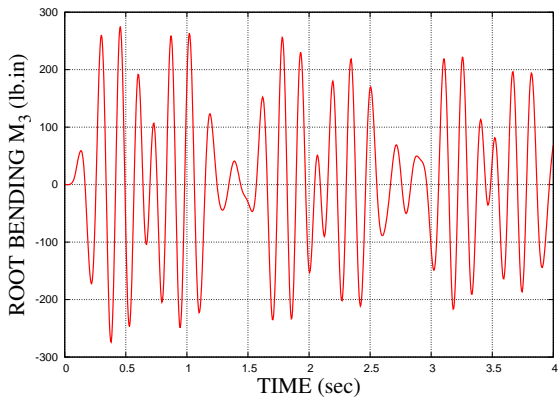
(a) F_1

(b) F_2

(c) F_3

(d) M_1

(e) M_2

(f) M_3

Figure 9: Stress resulant time histories at the root of a composite beam.

Legendre spectral elements are compared with the conventional 2nd order elements. Exponential convergence rates were observed as expected for this type of element. A composite cantilever beam were studied both statically and dynamically. The static results are verified against those obtained by Dymore. The elastic coupling effects were shown in these two cases. It concludes that BeamDyn is a powerful tool for composite beam analysis that can be used as a module in the FAST modularization framework.

Acknowledgments

References

[1] Wikipedia, "Wind power in the United States— Wikipedia, The Free Encyclopedia," 2013, [Online; accessed 10-June-2013].

[2] Reissner, E., "On one-dimensional large-displacement finite-strain beam theory," *Studies in Applied Mathematics LII*, 1973, pp. 87–95.

[3] Simo, J. C., "A finite strain beam formulation. The three-dimensional dynamic problem. Part I," *Computer Methods in Applied Mechanics and Engineering*, Vol. 49, 1985, pp. 55–70.

[4] Simo, J. C. and Vu-Quoc, L., "A three-dimensional finite-strain rod model. Part II," *Computer Methods in Applied Mechanics and Engineering*, Vol. 58, 1986, pp. 79–116.

[5] Jelenić, G. and Crisfield, M. A., "Geometrically exact 3D beam theory: implementation of a strain-invariant finite element for statics and dynamics," *Computer Methods in Applied Mechanics and Engineering*, Vol. 171, 1999, pp. 141–171.

[6] Betsch, P. and Steinmann, P., "Frame-indifferent beam finite elements based upon the geometrically exact beam theory," *International Journal for Numerical Methods in Engineering*, Vol. 54, 2002, pp. 1775–1788.

[7] Ibrahimbegović, A., "On finite element implementation of geometrically nonlinear Reissner's beam theory: three-dimensional curved beam elements," *Computer Methods in Applied Mechanics and Engineering*, Vol. 122, 1995, pp. 11–26.

[8] Ibrahimbegović, A. and Mikdad, M. A., "Finite rotations in dynamics of beams and implicit time-stepping schemes," *International Journal for Numerical Methods in Engineering*, Vol. 41, 1998, pp. 781–814.

[9] Cook, R. D., Malkus, D. S., Plesha, M. E., and Witt, R. J., *Concepts and Applications of Finite Element Analysis*, Wiley, 4th ed., 2001.

[10] Yu, W. and Blair, M., "GEBT: A general-purpose nonlinear analysis tool for composite beams," *Composite Structures*, Vol. 94, 2012, pp. 2677–2689.

[11] Wang, Q., Yu, W., and Sprague, M. A., "Geometric nonlinear analysis of composite beams using Wiener-Milenković parameters," *Proceedings of the 54th Structures, Structural Dynamics, and Materials Conference*, Boston, Massachusetts, April 2013.

[12] Hodges, D. H., *Nonlinear Composite Beam Theory*, AIAA, 2006.

[13] Patera, A. T., "A spectral element method for fluid dynamics: Laminar flow in a channel expansion," *Journal of Computational Physics*, Vol. 54, 1984, pp. 468–488.

[14] Ronquist, E. M. and Patera, A. T., "A Legendre spectral element method for the Stefan problem," *International Journal for Numerical Methods in Engineering*, Vol. 24, 1987, pp. 2273–2299.

[15] Deville, M. O., Fischer, P. F., and Mund, E. H., *High-order Methods for Incompressible Fluid Flow*, Cambridge University Press, 2002.

[16] Komatitsch, D. and Vilotte, J. P., "The spectral element method: and efficient tool to simulate the seismic response of 2D and 3D geological structures," *Bulletin of the Seismological Society of America*, Vol. 88, 1998, pp. 368–392.

[17] Sridhar, R., Chakraborty, A., and Gopalakrishnan, S., "Wave propagation in anisotropic and inhomogeneous untracked and cracked structures using the pseudo spectral finite element method," *International Journal of Solids and Structures*, Vol. 43, 2006, pp. 4997–5031.

[18] Sprague, M. A. and Geers, T. L., "A spectral-element method for modeling cavitation in transient fluid-structure interaction," *International Journal for Numerical Methods in Engineering*, Vol. 60, 2004, pp. 2467–2499.

[19] Ben-Tal, A., Bar-Yoseph, P. Z., and Flashner, H., "Optimal maneuver of a flexible arm by space-time finite element method," *Journal of Guidance, Control, and Dynamics*, Vol. 18, 1995, pp. 1459–1462.

[20] Ben-Tal, A., Bar-Yoseph, P. Z., and Flashner, H., "Space-time spectral element method for optimal slewing of a flexible beam," *International Journal for Numerical Methods in Engineering*, Vol. 39, 1996, pp. 3101–3121.

[21] Kudela, P., Krawczuk, M., and Ostachowicz, W., "Wave propagation modeling in 1D structures using spectral finite elements," *Journal of Sound and Vibration*, Vol. 300, 2007, pp. 88–100.

[22] Sprague, M. A. and Geers, T. L., "Legendre spectral finite elements for structural dynamics analysis," *Communications in Numerical Methods in Engineering*, Vol. 24, 2008, pp. 1953–1965.

[23] Zrahia, U. and Bar-Yoseph, P., "Plate spectral elements based upon Reissner-Mindlin theory," *International Journal for Numerical Methods in Engineering*, Vol. 38, 1995, pp. 1341–1360.

[24] Kudela, P., Zak, A., Krawczuk, M., and Ostachowicz, W., "Modeling of wave propagation in composite plates using the time domain spectral element method," *Journal of Sound and Vibration*, Vol. 302, 2007, pp. 728–745.

[25] Sprague, M. A. and Brito, K. D., "Reissner-Mindlin Legendre spectral finite elements with mixed reduced quadrature," *Finite Elements in Analysis and Design*, Vol. 58, 2012, pp. 74–83.

[26] Wang, Q. and Sprague, M. A., "A Legendre spectral finite element implementation of geometrically exact beam theory," *Proceedings of the 54th Structures, Structural Dynamics, and Materials Conference*, Boston, Massachusetts, April 2013.

[27] Jonkman, J. M., "The new modularization framework for the FAST wind turbine CAE tool," *Proceedings of the 51st AIAA Aerospace Sciences Meeting including the New Horizons Forum and Aerospace Exposition*, Grapevine, Texas, January 2013.

[28] Bauchau, O. A., *Flexible Multibody Dynamics*, Springer, 2010.

[29] Bauchau, O. A., Epple, A., and Bottasso, L., "Scaling of Constraints and Augmented Lagrangian Formulations in Multibody Dynamics Simulations," *Journal of Computational and Nonlinear Dynamics*, Vol. 4, 2009, pp. 021007–1–9.

American Institute of Aeronautics and Astronautics

[30]Chung, J. and Hulbert, G. M., "A time integration algorithm for structural dynamics with improved numerical dissipation: the generalized-α method," *Journal of Applied Mechanics*, Vol. 60, 1993, pp. 371–375.

[31]Xiao, N. and Zhong, H., "Non-linear quadrature element analysis of planar frames based on geometrically exact beam theory," *International Journal of Non-Linear Mechanics*, Vol. 47, 2012, pp. 481–488.

[32]Mayo, J. M., García-Vallejo, D., and Domínguez, J., "Study of the geometric stiffening effect: comparison of different formulations," *Multibody System Dynamics*, Vol. 11, 2004, pp. 321–341.

[33]Yu, W., Hodges, D. H., Volovoi, V., and Cesnik, C. E. S., "On Timoshenko-Like modeling of initially curved and twisted composite beams," *International Journal of Solids and Structures*, Vol. 39, 2002, pp. 5101–5121.

[34]Wang, Q. and Yu, W., "Asymptotic multi physics modeling of composite slender structures," *Smart Materials and Structures*, Vol. 21, 2012, pp. 035002.